



Investigation of oxide scale adhesion on hot-rolled steel using the tensile test and acoustic emission

Seksan SINGTHANU¹, Prayoon SURIN¹, Manop PIPATHATTAKUL¹, and Thanasak NILSONTHI^{2,*}

¹ Faculty of Engineering, Pathumwan Institute of Technology, 833 Rama1 Road, Wang Mai, Pathumwan, Bangkok, 10330, Thailand

² High Temperature Corrosion Research Centre and Department of Materials and Production Technology Engineering, Faculty of Engineering, King Mongkut's University of Technology North Bangkok, 1518, Pracharat 1 Road, Wongsawang, Bangsue, Bangkok, 10800, Thailand

*Corresponding author e-mail: thanasak.n@eng.kmutnb.ac.th

Received date:

29 December 2022

Revised date

4 April 2023

Accepted date:

8 May 2023

Keywords:

Tensile test;
Acoustic emission;
Oxide scale
Adhesion;
Hot-rolled steel coil

Abstract

This article addresses applying a tensile test with a CCD camera to assess scale adhesion on hot-rolled steel as a function of hot-rolled coil position. The scale adhesion in this study was shown in the value of the strain initiating the first scale spallation. The result of strain initiating the first scale spallation was confirmed with an acoustic emission (AE) method. The as-received hot-rolled coil was studied at the head, middle, and tail positions. A scanning electron microscope (SEM) and X-ray diffraction (XRD) were used to examine the scale morphology and phase identification respectively. The results show that the oxide scale comprises hematite and magnetite layers. It was found that the higher strain initiating the first scale spallation was revealed on the scale formed on the hot-rolled coil at the head and middle positions. This indicates that the oxide scale was more difficult to remove than at the tail position of the coil. The scale growth and cooling affects the stresses on the oxide layer and the steel substrate. A thin oxide layer on tail position of the hot-rolled coil will easily first crack and then buckle and followed by spallation, while a thick scale on head and middle positions of the hot-rolled coil was harder than that thin scale.

1. Introduction

Hot-rolled steel is the downstream steel industry. The hot-rolled steel strips is obtained from the slab through the hot-rolling process to reduce the thickness at a temperature of about 1,100°C to 1,250°C with a rolling or a large rolling platform, and then cooled by passing through cooling water. The steel passes into the coiling machine at a temperature of about 550°C to 710°C. The resulting hot-rolled steel strips will have a black surface and be in the form of a coil, called a "hot-rolled coil". The black surface cover on steel is an oxide scale. Black hot-rolled steel coil will be convenient for storage and transportation. If a surface quality is required the black scale must be completely removed by pickling in an acid solution during the descaling process. The hot-rolled steel can be used as a raw material in the production of various downstream industries such as automotive, machine, tube, containers, etc. The final thickness of the strip is determined according to the product specifications. The thickness of steel is reduced via the hot rolling line at temperature above the recrystallization temperature. Surface defects such as scale always form on the hot-rolled steel surface when exposed to a high temperature. Oxide-iron scale is primarily produced when the hot surface is oxidized by air [1-13]. Scale on the steel surface is typically removed by using a water jet during the hot-rolling process and hydrochloric acid after the process. Significant factors affecting scale formation include alloying elements [14-18], process temperature [19-21], atmosphere,

rolling speed, reduction per pass, etc. Alloying elements in steel enhance the mechanical properties of the material. Steel is an alloy of iron, silicon, manganese, carbon, copper, and a small amount of other elements, giving it high elasticity, strength, durability, and impact resistance. These alloying elements in steel affect the formation and adhesion of scale on hot-rolled steel. Such as silicon alloying in steel will result in a decrease in the oxidation rate and an increase in the adhesion of scale on the steel substrate, or copper alloys will decrease the oxidation rate and reduce scale adhesion. Scale adhesion is lowered and the scale thickness is increased with a higher finishing temperature. The water vapor atmosphere lessens scale adherence to a steel substrate during oxidation. One important factor for evaluating scale removal is scale adhesion. However, relatively no studies have been reported on the effect of hot-rolled coil position on scale adhesion. This research is focused on studying adhesion at the steel-scale interface of hot-rolled steel in the role of hot-rolled coil position. The tensile test and acoustic emission (AE) have been applied to investigate scale adhesion on the hot-rolled steel during the tensile load. For the tensile test, this is used with a CCD camera to visualize the scale spallation on the hot-rolled steel substrate. For acoustic emission, this is used to confirm when the first scale spallation occurred. Because the image of scale spallation from the CCD camera can only be focused on a small area in the center of the specimen, AE is used to confirm that the scale is the correct first spallation. The adhesion of scale in this research is represented by strain initiating the first scale spallation.

2. Experimental

2.1 Materials

Hot-rolled steel as received from steel industries with 8 mm thick is used in this study. The chemical composition of hot-rolled low carbon steel is 0.138 wt% C, 0.441 wt% Mn, 0.044 wt% Al, 0.010 wt% Cu, 0.006 wt% Si, 0.017 wt% P, and 0.009 wt% S. In Figure 1, the hot-rolled coil's head, middle, and tail positions are indicated for observation. The specimen is taken from the hot-rolled coil acquired from a slab made via the blast-furnace route. A hot rolling process is used with a finishing temperature of 790°C and a coiling temperature of 580°C. The oxide scale thickness of the as-received hot-rolled steel strips at the head position is $34 \pm 2.63 \mu\text{m}$, the middle position is $17 \pm 2.29 \mu\text{m}$, and the tail position is $10 \pm 1.15 \mu\text{m}$. The tensile strength of the steel at the head position is 429 MPa, at middle position is 427 MPa, and at tail position is 380 MPa.

2.2 Characterization

In addition to experimental procedures, these instruments allow for the analysis of experimental data with appropriate instruments. A scanning electron microscope (SEM) with energy dispersive spectrometer (EDS), (Quanta 450) is used to observe scale morphology and analyze the composition. The electron beam strikes over the steel surface and takes the scattered signal back to form an image. Energy X-rays up to 20 kV for energy dispersive spectrometer. Quantitative phase analysis can be obtained by X-ray diffraction (XRD), (Smart Lab). The X-ray is projected onto the steel surface and the X-ray diffraction is measured at different angles with an X-ray source of 1.2 kVA, Cu K- α 1, wavelength of 1.544 Å, tube voltage of 40 kV and tube current is 30 mA. The measured data indicates the type of metallic compound.

2.3 Adhesion test

A method to evaluate the scale adhesion on hot-rolled steel uses a tensile testing machine equipped with a CCD camera and an acoustic emission. It uses an Instron Model 5566 tensile testing machine with

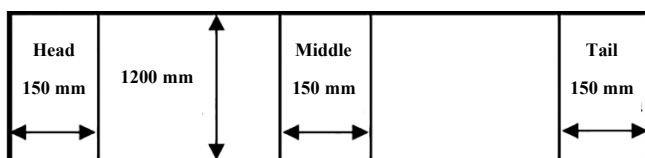


Figure 1. Position of the specimen within a hot-rolled coil selected for the study.

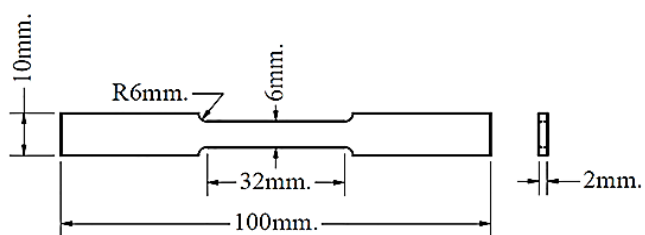


Figure 2. ASTM E8M standard specimen used for tensile testing.

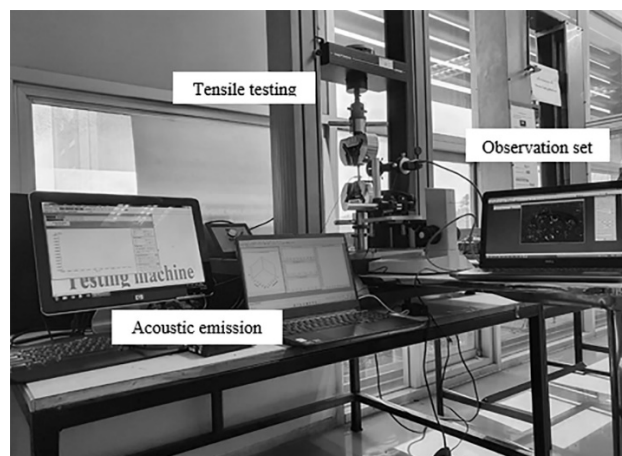


Figure 3. Tensile testing machine equipped with a set of observations and acoustic emission.

a 10 kN load. The test is performed at room temperature with a 0.04 s^{-1} of strain rate. The evolution of scale failure using a high-magnification lens in contact with a CCD camera. A resolution of $640 \text{ pixels} \times 480 \text{ pixels}$ is used for the video processing. The picture is captured under tensile loading using image framework programming. The tensile specimen is produced in accordance with the ASTM E8M standard. The specimen is a subsize specimen with 6 mm width, 100 mm length, and 25 mm gage length as shown in Figure 2. In order to use the tensile testing machine, the steel is thinned from 8 mm to 2 mm via horizontal milling machine. Figure 3 illustrates a tensile machine equipped with a set of observations and acoustic emission (AE). For acoustic emission, the data is continuously recorded by using AEWIN for USB AE node software. R15a small sensor produced by the physical acoustic corporation was applied to inspect the acoustic emission operation. This sensor is attached near the center of specimen. High-vacuum silicon grease is used to coat the sensor-sample interface for the best acoustic coupling. The USB AE node processing enhances the captured signals. A peak sensitivity of -63 to 80 dB with an operating frequency range of 50-400 kHz was used.

3. Results and discussion

3.1 Oxide scale structure

During the hot-rolling process, the steel surface was exposed to high-temperature oxidation. The initial reaction occurs at the scale-gas interface via mass transfer of oxygen, forming the oxide scale between the steel and the gas. Meanwhile, mass transfer of iron from the steel through the steel-scale interface into the oxide scale. Transport of iron and/or oxygen through the scale leads to a growing oxide scale. Metallographic examination of hot-rolled steel cross-sections exposed in the head, middle, and tail positions. It was shown that the very thick scale formed at the head position (Figure 4(a)). At the middle and tail positions (Figures 4(b-c)), the oxide scale thickness was less than that observed at the head position. Figure 5 shows the XRD results of the as-received hot-rolled coil at the head position (Figure 5(a)), middle position (Figure 5(b)), and tail position (Figure 5(c)). The scale was iron oxide as hematite (Fe_2O_3) and magnetite (Fe_3O_4), as detected by the X-ray diffractometer.

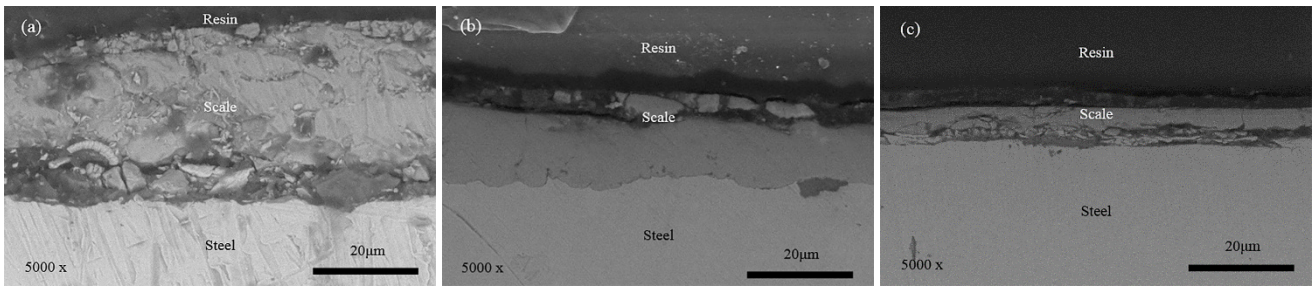


Figure 4. Metallographic cross-sections of the hot-rolled coil at head (a), middle (b), and tail (c) positions.

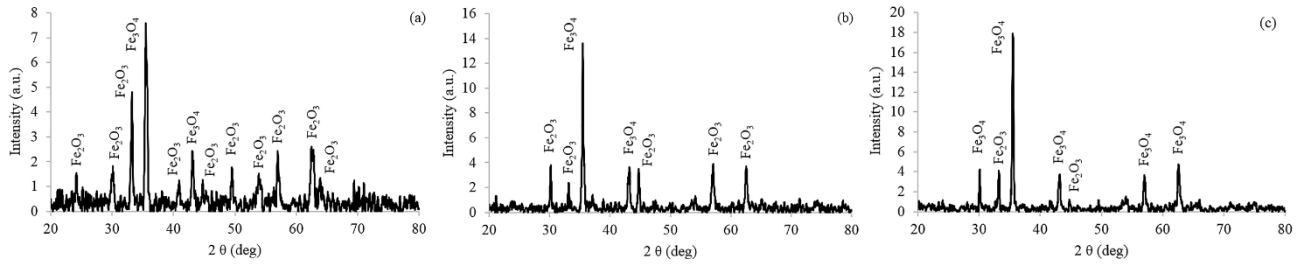


Figure 5. XRD patterns of the hot-rolled coil at head (a), middle (b), and tail (c) positions.

3.2 Adhesion of scale to hot-rolled steel

This research uses the tensile test and acoustic emission to investigate scale adhesion. The tensile test was used with a CCD camera to observe the scale adhesion on the hot-rolled steel, which was presented in scale spallation. However, this work uses acoustic emission to confirm when the first scale spallation occurred. From the stress–strain curve, it was seen that the tensile strength of the steel at the head position was 407 ± 10.26 MPa, at middle position was 431 ± 11.14 MPa, and at tail position was 326 ± 17.93 MPa. The adhesion of the oxide scale was described as increasing the scale thickness, compressive stress may also increase in the scale and result in localized spallation. Meanwhile, tensile stress will develop on the hot-rolled steel substrate. Under tensile stress, cracks appear when the elastic fracture strain was reached. Under compressive stress, the fracture damage at the interface leads to scale spallation. Evans [22,23] has reported that the stress was directly proportional to the thickness. The Fe_2O_3 and Fe_3O_4 on steel, in which the oxide layer was stressed in compression on cooling while the steel can be in tension. Evidence of the effect of stress on crack initiation has also been

found [24]. The higher crack density observed under creep-fatigue loadings with a compressive load was directly related to the mechanical behavior of the oxide scale. The strain at the first scale spallation and the spallation ratio can be analyzed after tensile test. Figure 6 shows strain initiating the first spallation and spallation ratio of the specimen with different positions in the hot-rolled coil. Strain initiating the first spallation defined as the first strain that scale spalled out from the surface of the steel during the tensile load. The spallation ratio was calculated by dividing the area where the scale spalled out by the total area of the image taken. Their value was received from video processing compared with data from a tensile test. It was found that the strain initiating the first spallation of the specimen at the head and middle positions was $4.15 \pm 0.17\%$ and $4.15 \pm 0.35\%$ respectively. This result was higher than the strain at the tail position, which was $2.07 \pm 0.74\%$. This indicates that the oxide scale formed on steel at the head and middle positions was strongly adhered to the steel. This might be due to the higher scale thickness producing higher compressive stress, causing the higher strain to initiate the first spallation during tension load.

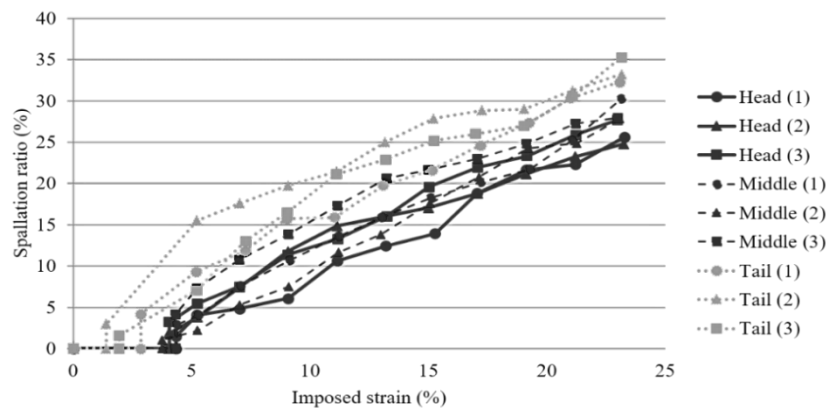


Figure 6. Strain initiating the first spallation and spallation ratio of the hot-rolled steel at head, middle and tail positions.

Data obtained from tensile testing with a CCD camera might be inaccurate due to the image capturing only the center of the specimen. This means that if the first scale spallation was out of focus, it will not be able to observe the first spallation of the scale. Therefore, the acoustic emission method can be used to support the result. Figure 7-9 shows acoustic emission (AE) occurrence as a function of the amplitude and time on the hot-rolled steel as a function of hot-rolled coil position. The acoustic emission exposes the sources of scale spallation during the tensile load. Acoustic emission will occur on the specimen on a periodic basis. AE activity under direct tension was significantly influenced by the hot-rolled coil position. At the head position, the concentrated AE signals initiated the higher waveform of 56.7 ± 5.13 dB with a time of 14.7 ± 0.52 s, corresponding to the strain initiating the first scale spallation at 4.15 ± 0.17 %. For the middle

position, the concentrated AE signals initiated the higher waveform of 56.0 ± 1.00 dB with a time of 14.7 ± 1.04 s, corresponding to the strain initiating the first scale spallation at 4.15 ± 0.35 %. For the tail position, the concentrated AE signals initiated the higher waveform of 71.3 ± 1.53 dB with a time of 7.8 ± 2.75 s, corresponding to the strain initiating the first scale spallation at 2.07 ± 0.74 %. It should be observed that the AE signals actually rarely wave under the elastic deformation region while waveforms were obviously seen under the plastic deformation region.

Table 1 presents the summary of data in a comprehensible and informative manner from the tensile test and acoustic emission method. This test was performed on a scale formed on the hot-rolled coil at different positions.

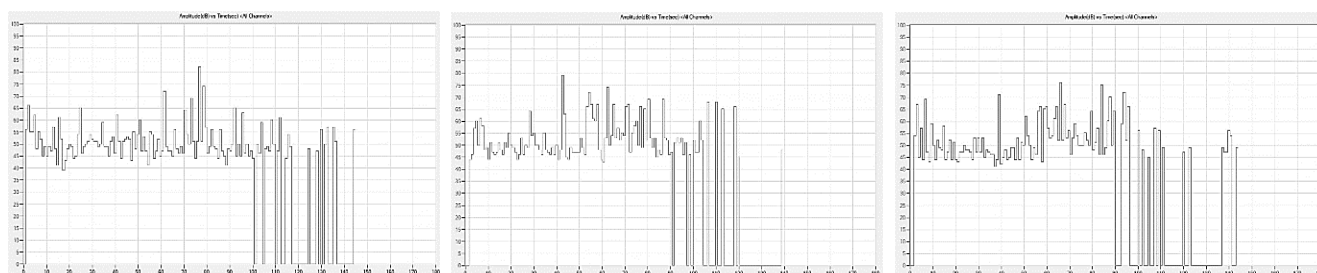


Figure 7. Incidence of acoustic emission on hot-rolled steel at the head position as amplitude (dB) with time (second).

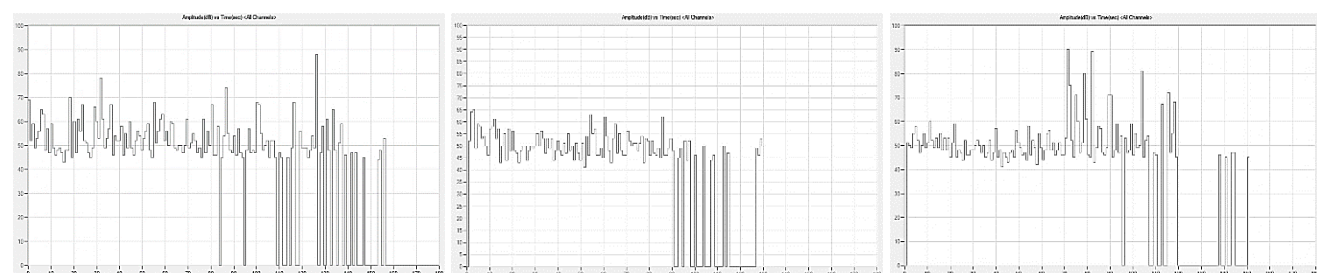


Figure 8. Incidence of acoustic emission on hot-rolled steel at the middle position as amplitude (dB) with time (second).

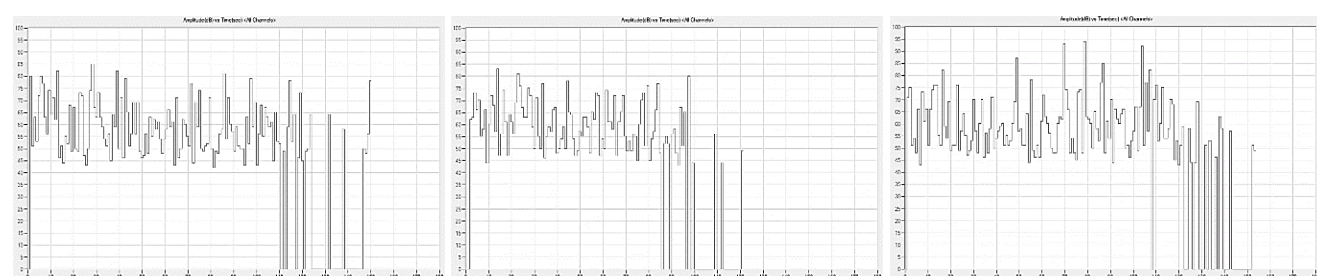


Figure 9. Incidence of acoustic emission on hot-rolled steel at the tail position as amplitude (dB) with time (second).

Table 1. Information from the tensile test with a CCD camera and acoustic emission method.

Scheme	Position of hot-rolled steel coil		
	Head	Middle	Tail
Scale thickness (μm)	34 ± 2.63	17 ± 2.29	10 ± 1.15
Type of scale in investigation		Fe_2O_3 and Fe_3O_4	
Strain initiating the first spallation (%)	4.15 ± 0.17	4.15 ± 0.35	2.07 ± 0.74
Time at strain initiating the first spallation (second)	14.7 ± 0.52	14.7 ± 1.04	7.8 ± 2.75
Amplitude of AE (dB)	56.7 ± 5.13	56.0 ± 1.00	71.3 ± 1.53

In this research, the role of the hot-rolled coil position in the adhesion of the oxide scale to hot-rolled steel was examined. The study found that most steels in the tail position showed lower scale adhesion and thickness. The result suggest that scale can be removed more easily than other coil position. This was a matter of discussion, compressively stressed oxide layers during oxide growth and cool-down were susceptible to spallation. A poorly adherent, thin layer will first buckle and subsequently spall when tensile cracks develop in regions of tensile stress and lead to spallation. Stresses develop in both an oxide and a steel substrate during temperature changes, corresponding to a difference in the thermal expansion coefficients between oxide and steel. Usually, more stress was developed in the steel than the oxide, so that the oxide was under compressive stress and the metal was under tensile stress during cooling. The average stress level was defined by the Tien-Davidson equation [25]. For thick oxide relative to the metal substrate, the average stress in the oxide layer (1) and the metal average stress (2) was given by

$$\sigma_{ox} = -\frac{E_{ox}\Delta T(\alpha_m - \alpha_{ox})}{(1-\vartheta)\left(1 + \frac{E_{ox}\varphi}{E_m h}\right)} \quad (1)$$

$$\sigma_m = +\frac{E_m\Delta T(\alpha_m - \alpha_{ox})}{(1-\vartheta)\left(1 + \frac{E_{ox}h}{E_m\varphi}\right)} \quad (2)$$

Here, $\Delta T = (T_{ox} - T)$, h as half the specimen thickness, φ the oxide thickness, E the appropriate Young's modulus, ϑ the Poisson ratio. For thin oxide relative to the metal substrate, the equation can be given by

$$\sigma_{ox} = -\frac{E_{ox}\Delta T(\alpha_m - \alpha_{ox})}{(1-\vartheta)} \quad (3)$$

$$\sigma_m = +\frac{E_m^2\Delta T\varphi(\alpha_m - \alpha_{ox})}{(1-\vartheta)(1 + E_{ox}h)} \quad (4)$$

Under the oxide layer of this research, it has been seen that compressive stress within the oxide can readily produce through-scale cracking and lead to spallation. A thin oxide layer will easily first crack and then buckle and lead to spallation, while a thick scale was harder than that thin scale. For this reason, it was a matter of discussion as to why the scale adhesion was decreasing for the hot-rolled coil at the tail position due to low scale thickness. At the head and middle positions, it can be seen that the scale adhesion was increased due to the high scale thickness.

Finally, the study of the scale adhesion of hot-rolled coil must continue to be studied in order to better understand. This research focuses on the effect of position in the hot-rolled coil for assessing scale adhesion as shown in strain initiating the first scale spallation. This information can be useful for the hot-rolled steel industry.

4. Conclusions

The tensile test and acoustic emission method were developed to assess the scale adhesion on hot-rolled steel as a function of hot-rolled coil position. The adhesion of the scale was represented by the strain initiating the first scale spallation. The scale on as-received

hot-rolled steel consists of hematite and magnetite. A higher strain initiating the first scale spallation was observed in the head and middle positions. This indicates higher-scale adhesion to hot-rolled coils at their positions. This may imply that scale was harder to descale at the head and middle positions than at the tail position. This was due to the stresses produced in the oxide and the steel as a result of scale growth and cooling.

Acknowledgements

This research was funded by National Science, Research and Innovation Fund (NSRF), and King Mongkut's University of Technology North Bangkok with Contract no. KMUTNB-FF-65-09. Sahaviriya Steel Industries Public Company Limited was responsible for hot-rolled steel.

References

- [1] P. Kofstad, *High temperature corrosion*. Elsevier Applied Science, London, 1988.
- [2] R. Y. Chen, and W. Y. D. Yuen, "Oxide-scale structures formed on commercial hot-rolled steel strip and their formation mechanisms," *Oxidation of Metals*, vol. 56, no. 1/2, pp. 89-118, 2001.
- [3] R. Y. Chen, and W. Y. D. Yuen, "Oxidation of low-carbon, low-silicon mild steel at 450-900°C under conditions relevant to hot-strip processing," *Oxidation of Metals*, vol. 57, no. 1/2, pp. 53-79, 2002.
- [4] R. Y. Chen, and W. Y. D. Yuen, "Review of the high-temperature oxidation of iron and carbon steels in air or oxygen," *Oxidation of Metals*, vol. 59, no. 5/6, pp. 433-468, 2003.
- [5] R. Y. Chen, and W. Y. D. Yuen, "Examination of oxide scales of hot rolled steel products," *Iron and Steel Institute of Japan International*, vol. 45, no. 1, pp. 52-59, 2005.
- [6] P. Sarrazin, A. Galerie, and J. Fouletier, *Les mécanismes de la corrosion sèche: une approche cinétique*. France: EDP Science, 2000.
- [7] P. Sarrazin, A. Galerie, and J. Fouletier, *Mechanisms of high temperature corrosion: a kinetic approach*. Zürich: Materials Science Foundations, Trans Tech Publications, 2008.
- [8] M. J. L. Gines, G. J. Benitez, T. Perez, E. Merli, M. A. Firpo, and W. Egli, "Study of the picklability of 1.8 mm hot-rolled steel strip in hydrochloric acid," *Latin American Applied Research*, pp. 281-288, 2002.
- [9] Z. Y. Jiang, A. K. Tieu, W. H. Sun, J. N. Tang, and D. B. Wei, "Characterisation of thin oxide scale and its surface roughness in hot metal rolling," *Materials Science and Engineering A*, vol. 435-436, pp. 434-438, 2006.
- [10] L. Suárez, R. Petrov, L. Kestens, M. Lamberigts, and Y. Houbaert, "Texture evolution of tertiary oxide scale during steel plate finishing hot rolling simulation tests," *Materials Science Forum*, vol. 550, pp. 557-562, 2007.
- [11] M. Zhang, and G. Shao, "Characterization and properties of oxide scales on hot-rolled strips," *Materials Science and Engineering A*, vol. 452-453, pp. 189-193, 2007.

- [12] Y. -L. Yang, C. -H. Yang, S. -N. Lin, C. -H. Chen, and W. -T. Tsai, "Effects of Si and its content on the scale formation on hot-rolled steel strips," *Materials Chemistry and Physics*, vol. 112, pp. 566-571, 2008.
- [13] A. Segawa, "Reproduction and deformation characteristics of oxide scale in hot rolling using vacuum rolling mill," *Materials Science Forum*, vol. 96, pp. 150-155, 2011.
- [14] S. Chandra-ambhorn, T. Phadungwong, and K. Sirivedin, "Effects of carbon and coiling temperature on the adhesion of thermal oxide scales to hot-rolled carbon steels," *Corrosion Science*, vol. 115, pp. 30-40, 2017.
- [15] S. Chandra-ambhorn, T. Nilsonthi, Y. Wouters, and A. Galerie, "Oxidation of simulated recycled steels with 0.23 and 1.03 wt.% Si in Ar-20% H₂O at 900°C," *Corrosion Science*, vol. 87, pp. 101-110, 2014.
- [16] R. Y. Chen, and W. Y. D. Yuen, "Isothermal and step isothermal oxidation of copper-containing steels in air at 980-1220°C," *Oxidation of Metals*, vol. 63, no. 3/4, pp. 145-168, 2005.
- [17] S. Chandra-ambhorn, A. Jutilartavorn, and T. Rojhirunsakool, "High temperature oxidation of irons without and with 0.06 wt% Sn in dry and humidified oxygen," *Corrosion Science*, vol. 148, pp. 355-365, 2019.
- [18] S. Chandra-ambhorn, and K. Ngamkham, "High temperature oxidation of micro-alloyed steel and its scale adhesion," *Oxidation of Metals*, vol. 88, pp. 291-300, 2017.
- [19] R. Y. Chen, and W. Y. D. Yuen, "A study of the scale structure of hot-rolled steel strip by simulated coiling and cooling," *Oxidation of Metals*, vol. 53, no. 5/6, pp. 539-560, 2000.
- [20] R. Y. Chen, and W. Y. D. Yuen, "Copper enrichment behaviours of copper-containing steels in simulated thin-slab casting processes," *Iron and Steel Institute of Japan International*, vol. 45, no. 6, pp. 807-816, 2005.
- [21] S. Chandra-ambhorn, K. Ngamkham, and N. Jiratthanakul, "Effects of process parameters on mechanical adhesion of thermal oxide scales on hot-rolled low carbon steels," *Oxidation of metals*, vol. 80, no. 1, pp. 61-72, 2013.
- [22] H. E. Evans, "Stress effects in high temperature oxidation of metals," *International Materials Reviews*, vol. 40, no. 1, pp. 1-40, 1995.
- [23] H. E. Evans, "Spallation of oxide from stainless steel AGR nuclear fuel cladding: mechanisms and consequences," *Materials Science and Technology*, vol. 4, pp. 415-420, 1988.
- [24] B. A. Kschinka, and J. F. Stubbins, "Creep-fatigue-environment interaction in a bainitic 2.25wt.%Cr-1wt.%Mo steel forging," *Materials Science & Engineering A*, vol. 110, pp. 89-102, 1989.
- [25] J. K. Tien, and J. M. Davidson, *Stress effects and the oxidation of metals*. ed J. V. Cathcart, New York, AIME, 1975.